Polymer Chemistry

Accepted Manuscript

This is an *Accepted Manuscript*, which has been through the Royal Society of Chemistry peer review process and has been accepted for publication.

Accepted Manuscripts are published online shortly after acceptance, before technical editing, formatting and proof reading. Using this free service, authors can make their results available to the community, in citable form, before we publish the edited article. We will replace this *Accepted Manuscript* with the edited and formatted *Advance Article* as soon as it is available.

You can find more information about *Accepted Manuscripts* in the Information for Authors.

Please note that technical editing may introduce minor changes to the text and/or graphics, which may alter content. The journal's standard Terms & Conditions and the Ethical guidelines still apply. In no event shall the Royal Society of Chemistry be held responsible for any errors or omissions in this *Accepted Manuscript* or any consequences arising from the use of any information it contains.

ROYAL SOCIETY OF CHEMISTRY

www.rsc.org/polymers

Journal Name

RSCPublishing

ARTICLE

Effect of molecular composition and crosslinking on adhesion of a bio-inspired adhesive

Cite this: DOI: 10.1039/xoxxoooooox

Juan Yang[a], Jaap Keijsers[a], Maarten van Heek[a], Anthonie Stuiver[b], Martien A. Cohen Stuart[a], Marleen Kamperman[a]

Received ooth January 2012,
Accepted ooth January 2012

DOI: 10.1039/xoxxoooooox

www.rsc.org/

In this article, catechol-functionalized polymers are synthesized by free radical polymerization of dopamine methacrylamide (DMA) and 2-methoxyethyl methacrylate (MEA) at 60 °C in DMF. By varying the DMA content in the polymer, it is found that during free radical polymerization, the catechol groups in DMA react with the propagating radicals, resulting in the formation of a crosslinked structure. We systematically study the effect of DMA content and crosslinking on the adhesion properties of the polymers. Under both dry and wet conditions, maximum adhesion is obtained for a polymer composed of 5 mol% DMA. This polymer exhibits an optimum balance between catechol content to strengthen the interface, compliance to ensure good contact formation and cohesive strength to resist separation. An increase in the crosslinking degree of the polymer resulted in reduced dry adhesion.

Introduction

The excellent underwater adhesion properties of marine organisms such as marine mussels[1, 2] and sabellariid polychaetes[3, 4] have attracted significant attention since decades. These marine organisms can achieve long-lasting and robust adhesion to various wet surfaces under harsh marine environments.[1, 5] It has been established that in holdfast proteins of several organisms, a significant amount of the catecholic amino acid L-3,4-dihydroxyphenylalanine (DOPA) is present, which contributes to the adhesion properties by forming strong covalent or non-covalent interactions with surfaces.[6-8]

The possible types and strengths of interactions between catechol and solid substrates have been extensively studied in the past few years. Liu et al. has summarized a full account of the different adhesion mechanisms.[9] Here only a few examples are listed. Frye reported that the catechol can react with organic silica to form organosilicon salts in which the silicon atom is in a penta-coordination form.[10] Lin and coworkers reported that DOPA in *Mytilus edulis* foot proteins-3 (mfp-3) interacts with mica by hydrogen bonding between the OH groups of catechol and the oxygen atoms in mica.[11] Several research groups studied the adsorption of catechol-conjugated polymers onto TiO_2 surfaces and different coordination bond configurations were proposed.[3, 5, 6, 12] The versatility of interactions between catechols and different surfaces provides the ability to strongly bind to substrates of widely varying composition.

Inspired by these versatile binding mechanisms of marine organisms, a lot of effort has been devoted to mimicking natural glues by using synthetic polymers incorporating catechol functionality.[13] One of the most common synthesis methods is to polymerize monomers bearing unprotected catechols by free radical polymerization. This method is facile because it is a one-step synthesis and the reaction conditions are not as stringent as with other polymerization techniques such as anionic polymerization.[14, 15] However, it is expected that this method is limited by the presence of the unprotected catechols, which are known to be radical scavengers.[16, 17] During polymerization, the catechol groups can interact with the propagating polymer radicals and may form a branched or cross-linked structure. Despite this expected limitation, many reports on the free radical polymerization of unprotected monomers exist in which the potential effect of catechols on the polymer structure is not mentioned.[18-23] The first synthesis of catechol-functionalized polymers from unprotected catechol-containing monomer has been described by Messersmith and co-workers.[24] N-methacrylated DOPA monomers were copolymerized with poly(ethylene glycol) diacrylate using either ultraviolet (UV) or visible light with a photoinitiator resulting in adhesive hydrogels. Three years later, they used thermally-initiated free radical polymerization to synthesize a random copolymer poly(dopamine methacrylamide-*co*-methoxyethyl acrylate) (p(DMA-*co*-MEA)) containing 11.3 mol% DMA.[18] The polymer was coated onto a poly(dimethyl siloxane) (PDMS) pillar array. It was found that wet adhesion

of the patterned surface increased 15-fold when coated with p(DMA-*co*-MEA). The adhesion of the coated structure was reversible and the adhesive strength decreased only slightly after 1000 cycles under both dry and wet conditions. A similar adhesion enhancement for patterned surfaces due to a p(DMA-*co*-MEA)-coating was observed by Washburn and coworkers.[19] Stewart and coworkers copolymerized dopamine methacrylamide with a phosphate based monomer: 2-(methacryloyloxy) ethyl phosphate. Combining the synthesized polymer with a second polymer bearing positive charges (e.g. protonated amine polymers) in the presence of divalent cations (Ca^{2+} or Mg^{2+}) resulted in the formation of a polyelectrolyte complex.[21-23] This complex coacervate showed high underwater bond strength and may find use as biomedical adhesive.

These studies show that catechols accomplish strong and versatile interfacial interactions with different substrates and that the adhesion properties of synthetic catechol-containing polymers are promising. Therefore, one would expect that to increase the interfacial interactions the catechol content should be maximized. However, the performance of a pressure sensitive adhesive (PSA) is not only a function of its interfacial properties; the bulk mechanical properties are equally important. PSAs must be compliant and viscous to stick by simple contact, yet at the same time, must be resistant to creep, to avoid slow failure under load.[25] Therefore, the adhesion properties of catechol-containing polymers depend on the crosslinking of the polymer. As reported before, by introducing oxidant such as periodates, catechols are oxidized, and further undergo complicated crosslinking chemistry, yielding a crosslinked polymer network.[26] The altered bulk mechanical properties of the crosslinked polymer result in a different adhesion performance, as was shown by Wilker, et al, for poly[(3,4-dihydrostyrene)-*co*-styrene] (catechol content 33 mol%) systems.[6]

In this article, we systematically study the effect of catechol content in the polymer on the bulk mechanical and wet and dry adhesion properties. The potential influence of a crosslinked structure on the adhesion properties is also taken into account. Mechanical properties are measured with dynamic mechanical analysis and rheometry and the adhesion properties are studied by indentation adhesion tests.

Experimental

Materials

Dopamine hydrochloride, methacrylic anhydride (94%), 2-methoxyethyl acrylate (98%), basic alumina, deuterochloroform (99.96%), tetrahydrofuran (98.5%), ethyl acetate (99%), dimethylformamide (99.8%), 2,2'-Azobis(2-methylpropionitrile) (98%), dichloromethane (98.5%), methanol (98.5%), 3,4-dimethoxyphenethyl amine (97%) and triethylamine (>99.5%) were purchased from Sigma-Aldrich. Sodium hydroxide solution (1 M) and anhydrous magnesium sulfate ($MgSO_4$, 97%) were purchased from Merck. Hydrochloride solution (1 M) was purchased from Fluka. Hexane (p.a.) and diethyl ether (p.a.) were purchased from Biosolve. Sodium tetraborate decahydrate (p.a.) and sodium bicarbonate were purchased from J.T.Baker.

Monomer synthesis

Dopamine methacrylamide (DMA) was synthesized by reaction of dopamine hydrochloride and methacrylic anhydride in a mixture of tetrahydrofuran (THF) and Milli-Q water, see Scheme 1.[19] 30 g of sodium borate tetrahydrate and 12 g of sodium bicarbonate were added to 300 ml Milli-Q water. The aqueous solution was bubbled with N_2 for 20 min, followed by addition of 15 g of dopamine hydrochloride. Next, 14.1 ml of methacrylic anhydride in 75 ml of THF was added dropwise. The pH of the solution was maintained above 8 by adding drops of 1 M NaOH solution. The reaction mixture was stirred overnight (around 14 h) under continuous N_2 bubbling at room temperature. After the reaction, a slightly pinkish slurry was formed with a white solid present at the bottom of the flask. The reaction mixture was filtered by vacuum filtration and the residue, a clear slightly pinkish solution, was washed twice with 150 ml ethyl acetate. The obtained aqueous solution was acidified by 1 M HCl to a pH of around 2, followed by extraction with 150 ml ethyl acetate for three times. The brownish organic solution obtained from extraction was collected and dried over $MgSO_4$. Afterwards, the volume of the solution was reduced to around 80 ml by rotary evaporation and precipitated into 800 ml hexane. The formed suspension was stored at 4 °C overnight to aid crystallization. After 14 h, the resulting brownish solids were collected, dissolved in 100 ml ethyl acetate and precipitated in 1000 ml hexane. The final solid obtained by filtration of the suspension was dried in a vacuum oven overnight at room temperature and the yield was 54%. ^{1}H NMR (400 MHz, d-DMSO, δ (ppm)): 6.62-6.42 (m, 3H, Ph), 5.92 (d, 1H, CH_2=C-), 5.27 (d, 1H, CH_2=C-), 3.23-3.18 (q, 2H, Ph-CH$_2$-CH_2-NH-), 2.55-2.51 (t, 2H, Ph-CH_2-CH$_2$-), 1.82 (s, 3H, CH$_2$=C(O)-CH_3). ^{13}C NMR (400 MHz, d-DMSO): δ = 167.26, 145, 143.44, 140.05, 130.25, 119.14, 118.69, 115.93, 115.43, 40.89, 34.55, 18.59.

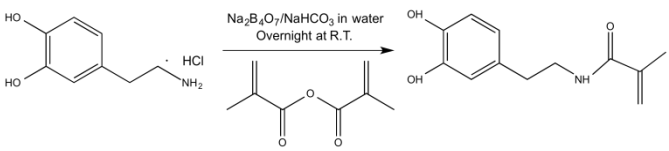

Scheme 1. Synthesis of DMA

Synthesis of poly(dopamine methacrylamide-co-2-methoxyethyl acrylate) p(DMA-*co*-MEA)

Five polymers with different compositions were obtained by varying the feed molar ratios of DMA and 2-methoxyethyl acrylate (MEA). The details of the polymers are described in Table 1. Polymers are denoted as P(DMA$_x$-*co*-MEA$_y$), where x and y are the molar percentages of DMA and MEA in the copolymer as obtained from ^{1}H NMR, respectively. Here, the synthesis of one typical copolymer is described in detail. Before polymerization, the inhibitor in MEA was removed by passing through a basic alumina column. 0.68 g DMA, 2.1 ml MEA and 42 mg of 2,2'-Azobis(2-methylpropionitrile) (AIBN) in 9.5 ml dimethylformamide (DMF) were added to a 50 ml three-neck round bottom flask, after which N_2 was bubbled through for 30 min. The reaction mixture was allowed to heat to 60 °C and was kept at this temperature for 3 h. The resulting viscous and slightly brownish mixture was diluted with 10 ml methanol, and added dropwise into 200 ml diethyl ether at 0 °C under continuous stirring. The resulting polymer was collected, dissolved in 15 ml dichloromethane and precipitated into 150 ml diethyl ether at 0 °C. After purification the polymer was dried in a vacuum oven overnight at room temperature. ^{1}H NMR (400 MHz, $CDCl_3$, δ (ppm)): 6.90-6.67 (m, 3H, Ph), 4.35 (b, 2H, -O-CH_2-CH$_2$-O-CH$_3$), 3.68 (b, 2H, -O-CH$_2$-CH_2-O-CH$_3$), 3.56 (b, 3H, -CH$_2$-CH$_2$-O-CH_3), 2.80-2.78 (br, 2H, -NH-CH$_2$-CH_2-Ph), 2.78-2.44 (br, 1H, -CH$_2$-CH(C=O)-CH$_2$-), 2.11-

1.65 (br, 2H, -CH_2-C(CH_3)-CH_2-CH(C=O)CH-), 1.44-1.11 (br, 2H, -CH_2-C(C=O)-CH_3).

Polymer characterization

All ^{1}H NMR and ^{13}C NMR measurements were carried out at 298 K on a Bruker AMX-400 spectrometer (400 MHz). Comparing the integrated area of the protons in the catechol and methoxy groups in DMA and MEA at chemical shift (δ) of 6.90-6.69 and 3.56, respectively, identified the DMA/MEA ratio in the final copolymer.

For the determination of the absolute molecular weight of the polymers and the weight-average number of branch points, a coupled size exclusion chromatography and multi-angle laser light scattering apparatus (SEC-MALLS) was used. Polymer samples (3 mg) were accurately weighed and dissolved overnight in 10 ml 0.02M potassiumtrifluoroacetate (KTFA) in 1,1,1,3,3,3-hexafluor-2-propanol (HFIP). Dissolved samples were filtered over a 0.45µm Teflon® filter prior to analysis. 0.02M potassiumtrifluoroacetate (KTFA) in 1,1,1,3,3,3-hexafluor-2-propanol (HFIP) was used as the mobile phase for SEC-MALLS. A 100µL sample was injected in a Viscotek system and separated over 2x PSS PFG analytical linear M GPC columns at 0.7 ml/min and 40 °C. The system was calibrated with a narrow standard PolyCAL PMMA 65kD (M_w=64,368, M_n=61,304). Data collection, system handling and calculations were done with OmniSEC software V4.6. The identification of the weight-average number of branch points in the polymer is based on a log-log intrinsic viscosity vs. molecular weight plot. According to the Mark-Houwink equation, for a polymer solution, the relation between intrinsic viscosity $[\eta]$ and molecular weight M is: $[\eta] = KM^a$, in which K and a are Mark-Houwink parameters. Therefore, we get $\log[\eta] = \log K + a\log M$. By fitting the data of $\log[\eta]$ and $\log M$ to the equation, we obtained $\log K$ and a as the intercept and slope, respectively. For a branched polymer, the branching ratio g' is used to describe the degree of branching of the polymer, which is the ratio of the intrinsic viscosity of the branched polymer, $[\eta]_{branched}$, and the linear polymer, $[\eta]_{linear}$: $g = [\eta]_{branched}/[\eta]_{linear}$. The degree of branching can also be expressed using g', which is defined as: $g' = R^2_{g,branched}/R^2_{g,linear}$, where R_g is the radius of gyration of the branched or linear polymer. The relation between g and g' is given the by shape factor ε: $g' = g^{\varepsilon}$. For many polymers, ε is typically 0.7-0.8. In our study, we used 0.75. g is then applied to derive the weight-average number of branch points per molecule using the Zimm-Stockmayer equation. The copolymers studied here are random, tri-functional, and polydisperse polymers. For this class of polymers, the Zimm-Stockmayer equation becomes:

$$g = \frac{6}{B_n}\left[\frac{1}{2}\left(\frac{2+B_n}{B_n}\right)^{1/2}\ln\left(\frac{(2+B_n)^{1/2}+{B_n}^{1/2}}{(2+B_n)^{1/2}-{B_n}^{1/2}}-1\right)\right] \quad (1)$$

where B_n is the weight-average number of branch points per molecule.[27]

The thermal behavior of the polymers was measured on a Perkin Elmer Diamond Differential Scanning Calorimeter (DSC), using a temperature range from -60 to 160 °C with a heating and cooling rate of 10 °C/min. Glass transition temperatures of the polymers were determined during heating. T_g was determined using the half heat capacity (C_p) extrapolation method. [28]

Polymer film preparation

For the adhesion test, optical microscopy, and AFM measurements, polymer films were prepared using a casting method. Square glass substrates, 26 mm long × 26 mm wide, were used as substrate for the polymer films. Glass substrates were washed with ethanol and acetone three times, and dried with N_2 prior to use. To prepare the polymer film, 0.3 g polymer was dissolved in 1 ml DMF and 0.3 ml of the solution was added onto the cleaned glass substrate. The solution completely wet the glass surface, after which the polymer film was dried in a vacuum oven at 50 °C. For the crosslinking study, 0.3 g polymer and different amounts of oxidants $NaIO_4$ were added to 1 ml DMF. Then 0.3 ml of the solution was spread immediately onto a cleaned glass substrate, which was left to dry under well-ventilated conditions for 24 h. Subsequently, the substrate was dried in a vacuum oven.

Optical microscopy

Cross-sections of the polymer films on the glass substrates were imaged using an Olympus BX 60. Images were obtained using a 10× magnification.

Atomic force microscopy

The roughness of the polymer films was analyzed using a Nanoscope V in Scan Asyst imaging mode, using nonconductive silicon nitride probes (Veeco, NY, U.S.A.) with a spring constant of 0.35 N/m. Images were recorded between 0.2 and 0.99 Hz and further processed with Nanoscope Analysis 1.20 software (Veeco Instruments Inc. 2010, U.S.A.).

Adhesion test

In adhesion tests, a 9.525 mm diameter glass sphere was fixed on a glass slide using Norland optical 61 adhesive and attached to a fixed stage. A thin polymer film was coated on a second glass slide and mounted to the stem of a Futek load cell (model LSB 200, S/N 454653 mated with USB210, S/N 454846, capacity: 250 g). The coupled actuator (Thorlabs Z825B) was connected to a controller (Thorlabs TDC001) to control the motion of the polymer film (a picture of the setup is shown in Figure S1). For all the measurements under both dry and wet conditions, the polymer film was indented at 0.01 mm/s until a predefined preload force was achieved. Subsequently, the polymer film and glass probe were allowed to be in contact for 300 s. The polymer film was then retracted at 0.01 mm/s and the adhesion force between the glass probe and polymer film was measured. Wet adhesion measurements were performed in aqueous hydrogen chloride solutions at pH 3. Before the measurement, the polymer film was immersed in the aqueous solution for at least one hour to completely swell the polymer films.

Dynamic mechanical analysis

Viscoelastic behavior of the polymers was studied with a TA instruments dynamic mechanical analyzer Q800. For polymer P($DMA_{0.25}$-co-$MEA_{0.75}$), a film tension clamp was used. The polymer was dissolved in chloroform, subsequently cast in a Teflon beaker and dried in a vacuum oven. The obtained polymer film was cut to rectangular specimens of 7.0 mm × 4 mm × 0.17 mm. For P($DMA_{0.05}$-co-$MEA_{0.95}$) and P($DMA_{0.10}$-co-$MEA_{0.90}$), a 8.65 mm diameter compression clamp was used. Polymer pieces were placed on the clamp after which a few drops of chloroform were added, which enabled the polymer to form a homogeneous sample of the right dimensions (4 mm height × 8.65 diameter). The sample was left to dry overnight under ambient conditions before measurements were carried out. Frequency sweeps from 100 to 0.01 Hz were performed to measure the storage modulus (G') and loss modulus (G'') at 26-

30 °C. Measurements were repeated after 8 hours and did not result in significant differences, indicating that most solvent had evaporated.

Rheometry

Rheological measurements were performed on the DHR3 Rheometer (TA instruments, US) equipped with a Peltier temperature control system. A plate of 8 mm diameter was used as top geometry while the Peltier serves as bottom geometry. We applied sinusoidal oscillations with a small constant deformation amplitude of 1% (which was tested to be in the linear regime) at an oscillation frequency of 1 Hz) and at a temperature specifically mentioned in the result part. To prepare the polymer samples, polymer PMEA was heated up to 90 °C in a vacuum oven and cooled down to room temperature. The resulting cylindrical sample with diameter of 8 mm was subsequently squeezed between the plates.

RESULTS AND DISCUSSION

1 Polymerization

We synthesized copolymers p(DMA-*co*-MEA) with different molar ratios of the two monomers DMA and MEA (Table 1) by free radical polymerization using DMF as solvent. DMF, which is polar, yet aprotic was chosen to reduce the ability of catechols to donate hydrogens to scavenge free radicals during polymerization. In a polar solvent such as DMF, catechols may interact with DMF by forming hydrogen bonds, thereby limiting, to some extent, the interaction between catechols with propagating radicals. It is important to avoid the use of protic polar solvents such as methanol, which can also form hydrogen bonds with surrounding methanol molecules. For these solvents, the hydrogen atom donating behavior of catechols to scavenge free radicals is not reduced.[16, 17]

The chemical compositions of the final polymers were identified by comparing the integrated area of the protons of the catechol and methoxy groups in DMA and MEA at chemical shifts (δ) 6.90-6.69 and 3.56, respectively (see Figure S2). As shown in Table 1, the composition of DMA and MEA in the final polymer was somewhat different from the feed composition of the monomers, which may be due to the difference in monomer reactivity of DMA and MEA. The molecular weight M_n of the polymers became smaller when more DMA was added, which is possibly due to faster termination of the polymer chains by increased radical scavenging probabilities. The polydispersity index (PDI) of the polymers containing low amounts of DMA is around 2.0, which is typical for polymers synthesized using free radical polymerization. For P($DMA_{0.25}$-*co*-$MEA_{0.75}$), the PDI is 2.9, which is higher than those for polymers obtained from normal free radical polymerization. This higher PDI might be due to the still existing radical scavenging effect of catechols, which will be elucidated later.

During polymerization, the catechol groups in DMA were not protected. Although we tried to keep the scavenging ability to a minimum by using DMF, the propagating radicals in one polymer chain may still react with the catechol radicals in another polymer chain, so as to form a crosslinked structure.[29] The possibility of crosslinking was tested using SEC-MALLS by determining the weight-average number of branch points per polymer chain in the final polymer (see Figure S3). As shown in Table 1, with more incorporation of DMA, the number of branches in every polymer chain increased, although the number of branches in all the copolymers is small. Moreover, it was observed that polymers with a higher DMA content were more difficult to dissolve in common organic solvents. Homopolymer PDMA was insoluble in most common organic solvents and only showed limited solubility in DMF. Due to the limited solubility, PDMA could not be measured using SEC-MALLS. Yet the poor solubility is a clear indication that a crosslinked architecture is formed in PDMA. The number and position of crosslinks that were obtained during the free radical polymerization process are poorly controlled. Despite this lack of control, crosslinking may affect the adhesion performance of the polymers.[19] This will be discussed below. Scheme 2 shows a proposed crosslinking mechanism during the radical polymerization.

Table 1. Specifications of the synthesized polymers

	Feed molar ratio		Polymer			
	DMA	MEA	M_n [a]	M_w [b]	PDI[c]	B_n [d]
PMEA	0	1	54,946	95,440	1.7	0.041
P($DMA_{0.05}$-*co*-$MEA_{0.95}$)	1	19	64,397	121,867	1.9	0.12
P($DMA_{0.10}$-*co*-$MEA_{0.90}$)	1	5.7	61,634	124,589	2.0	0.18
P($DMA_{0.25}$-*co*-$MEA_{0.75}$)	1	2	37,331	106,784	2.9	0.31
PDMA	1	0	n.d.	n.d.	n.d.	n.d.

a: the number average molecular weight; b: the weight average molecular weight; c: polydispersity; d: weight-average number of branch points per molecule.

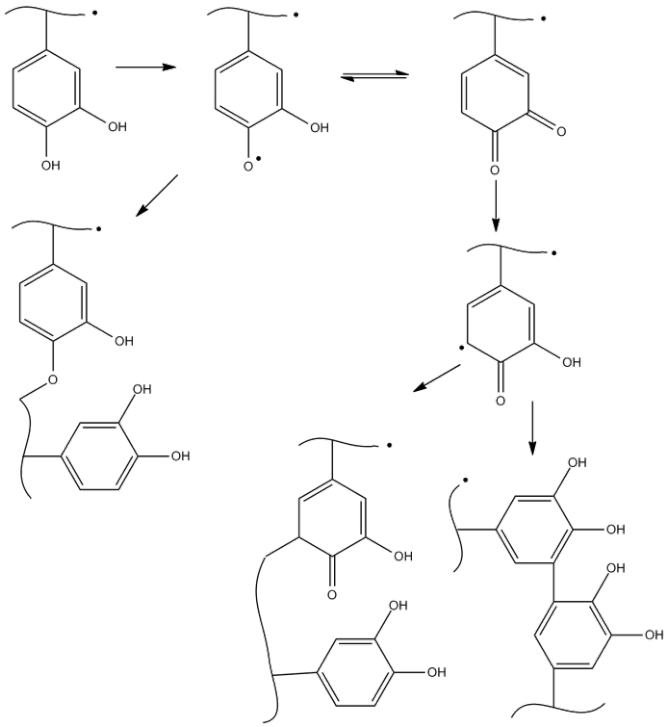

Scheme 2. Proposed crosslinking mechanism for the radical polymerization of vinyl monomers bearing unprotected catechols.[29]

More experiments need to be performed to verify this mechanism. However, it is challenging to perform mechanistic studies on these polymeric systems due to the small degree of crosslinking. A resulting architecture obtained from free radical polymerization of monomers MEA and DMA is proposed, as shown in Scheme 3.

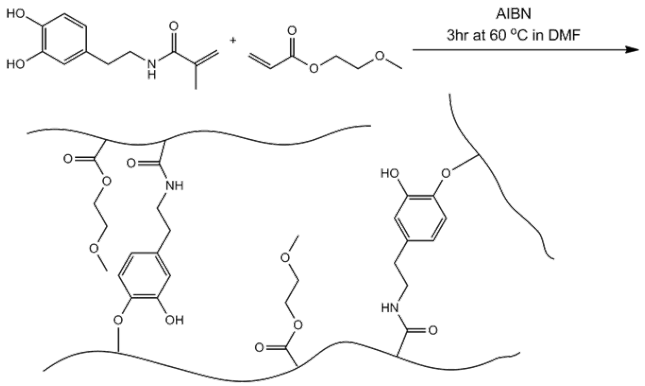

Scheme 3. Synthesis and a proposed resulting architecture of copolymer p(DMA-*co*-MEA)

To verify the crosslinked structure of PDMA, a second catechol-functionalized homopolymer was prepared by free radical polymerization of N-(3,4-dimethoxyphenethyl)acrylamide (NDMA) under the same polymerization conditions. In the new polymerization, methyl-protected catechols prohibit radical scavenging and linear polymer chains should be obtained.[13] The obtained polymer was demethylated using BBr_3 to free the catechol groups and linear PDMA (l-PDMA) was obtained. The synthesis and characterization details are given in the ESI and Figure S4.

Full characterization and property profiles of (co)polymers synthesized using protected catechol monomers will be the subject of a subsequent paper. PDMA and l-PDMA were dissolved in 0.1 mM NaOH solutions at pH = 10 under inert conditions. At this pH the catechols in the polymers should be partially deprotonated and the polymers charged and soluble in water. The solubility test showed that PDMA was insoluble while l-PDMA was soluble (Figure S5). We note that full deprotection of l-PDMA was not confirmed. However, partial deprotection would lower the solubility of l-PDMA in 0.1 mM NaOH, due to the hydrophobicity of the residual methoxy groups. Therefore, the strongly increased solubility of l-PDMA in 0.1 mM NaOH in comparison to PDMA verified the crosslinked structure of PDMA.

2 Mechanical properties of polymers

The mechanical properties of the polymers were measured by dynamic mechanical analysis (DMechA) and rheometry. DMechA is used as an abbreviation for dynamic mechanical analysis to differentiate it from dopamine methacrylamide. Due to the large variation in material properties different techniques and different measuring geometries were used. As shown in Table 2, PMEA was measured with rheometry using a compression geometry, while the copolymers of DMA and MEA were measured with DMechA using a compression clamp for P($DMA_{0.05}$-*co*-$MEA_{0.95}$) and P($DMA_{0.10}$-*co*-$MEA_{0.90}$), and a film tension clamp for P($DMA_{0.25}$-*co*-$MEA_{0.75}$). The choice of geometry for each measurement depended on the processability of the polymer and the required sample dimensions. For example, whereas PMEA flows at room temperature which precludes the use of a film tension clamp, P($DMA_{0.25}$-*co*-$MEA_{0.75}$) has a T_g at 33 °C, rendering the film tension clamp more appropriate than the compression clamp. For PDMA, the incorporation of only DMA without MEA resulted in very high T_g (> 160°C) for the polymer, which may be due to the presence of a benzene ring in DMA. The high T_g and the poor solubility of PDMA make this polymer so difficult to process that no proper dynamic mechanical analysis data could be obtained. Since the measurements were performed with different methods, geometries and temperatures, the storage and loss moduli obtained here should be regarded as an estimate of the polymer mechanical properties. Mechanical properties of the different polymer compositions at a frequency of 1 Hz are shown in Table 2.

Table 2. Mechanical properties of the polymer compositions

	Method used	Storage Modulus (kPa)	Loss Modulus (kPa)	Temperature measurement (°C)	Tan δ
PMEA	Rheometry	25	27	20	1.08
P($DMA_{0.05}$-*co*$MEA_{0.95}$)	DMechA, compression	229	84	29	0.37
P($DMA_{0.10}$-*co*-$MEA_{0.90}$)	DMechA, compression	230	130	30	0.56
P($DMA_{0.25}$-*co*-$MEA_{0.75}$)	DMechA, film tension	$4.8x10^4$	$3.7x10^3$	26	0.08
PDMA	n.d.	n.d.	n.d.	n.d.	n.d.

The overall polymer composition strongly influences the mechanical properties. The value of the storage modulus for a given temperature increased from tens to ten thousands of kPa by increasing the ratio of DMA to MEA from 0/100 to 25/75. Polymers with a glass transition temperature below room temperature (e.g. PMEA with T_g -36 °C) exhibit both a low storage modulus and a high damping factor (tan δ). In comparison, polymers with more DMA have a higher T_g (e.g. P($DMA_{0.25}$-*co*-$MEA_{0.75}$) with T_g 33 °C), exhibiting a higher storage modulus and a lower damping factor. Thus, PMEA shows significant viscoelastic behavior at room temperature, whereas P($DMA_{0.25}$-*co*-$MEA_{0.75}$) is stiff and elastic.

Small amounts of crosslinking can lead to drastic changes in the rheological behavior of polymer melts.[30] Typically, as the number of entanglements increases upon increasing the degree of crosslinking, the resistance to creep increases. However, for the set of polymers described here, not only crosslinking, but also the T_g and molecular weight vary significantly between polymers. Therefore, creep studies on a larger set of polymers would be needed to study the effect of crosslinking on the frequency dependence of the mechanical properties of P(DMA-*co*-MEA) copolymers.

3 Adhesion properties

To study the adhesion properties of the polymers under dry and wet conditions, a polymer film on a cleaned glass substrate for each polymer was prepared. The thickness for the five polymer films was similar to avoid substrate-induced artifacts on the indentation measurement results. The film thickness of the five samples was measured and listed in Table S1; a representative sample is shown in Figure 1.

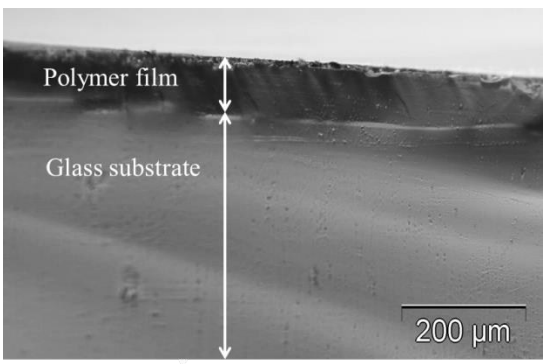

Figure 1. Optical microscopy image of (co)polymer on a pre-treated glass substrate. The thickness of the polymer layer was measured with optical microscopy (× 10 magnification).

The topography of the polymer films was imaged with AFM (Figure 2). The mean square roughness of the polymer films R_q was around 1 nm, which means that relatively homogeneous films were formed on the substrate.

The adhesion of the polymers under dry and wet conditions was measured by indentation adhesion tests. Figure 3 shows a typical force-time curve of P($DMA_{0.05}$-*co*-$MEA_{0.95}$) for dry adhesion. The pull-off force is obtained from the force-time curves and is defined as the maximum force required for debonding. The adhesion force as a function of preload force for dry adhesion is shown in Figure 4.

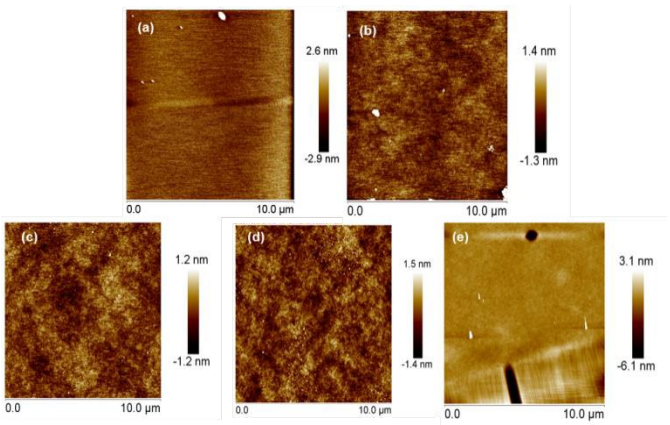

Figure 2. AFM topography images of a polymer film on a glass substrate. a) PMEA. Roughness average= 0.36 nm. b) P($DMA_{0.05}$-*co*-$MEA_{0.95}$). Roughness average= 1.3 nm. c) P($DMA_{0.10}$-*co*-$MEA_{0.90}$). Roughness average= 0.37 nm. d) P($DMA_{0.25}$-*co*-$MEA_{0.75}$). Roughness average= 0.4 nm. e) PDMA. Roughness average= 0.96 nm.

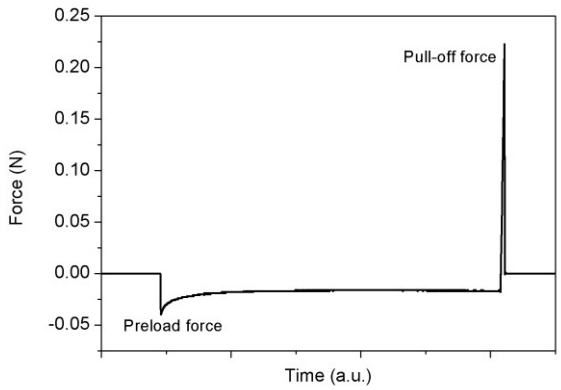

Figure 3. Typical curve of force as a function of time obtained from adhesion test. Positive loads are tensile and negative loads compressive.

Dry adhesion

In Figure 4, we compare dry adhesion strength for the various catechol-functionalized polymers. PMEA shows moderate dry adhesion in the investigated preload range from 0 to 35 mN. During the retraction step, a bundle of fibrils were observed between the probe and the polymer film and polymer residue was left on the probe, suggesting that in this case debonding occurred as cohesive failure. By incorporating 5 mol% of DMA into the polymer, P($DMA_{0.05}$-*co*-$MEA_{0.95}$ exhibited higher dry adhesion, with pull-off forces in the range of 0.06-0.2 N. By incorporating 10 mol% of DMA into the polymer, P($DMA_{0.10}$-*co*-$MEA_{0.90}$) exhibited decreased adhesion, with pull-off forces in the range of 0.015-0.05 N. A further increase in the DMA content, represented by P($DMA_{0.25}$-*co*-$MEA_{0.75}$) and PDMA, resulted in negligible adhesion. Therefore, in our set P($DMA_{0.05}$-*co*-$MEA_{0.95}$) is the optimal composition under dry conditions. DMA-containing polymers all show adhesive failure, without fibril-formation during the retracting step and without optically detectable residue left on the probe.

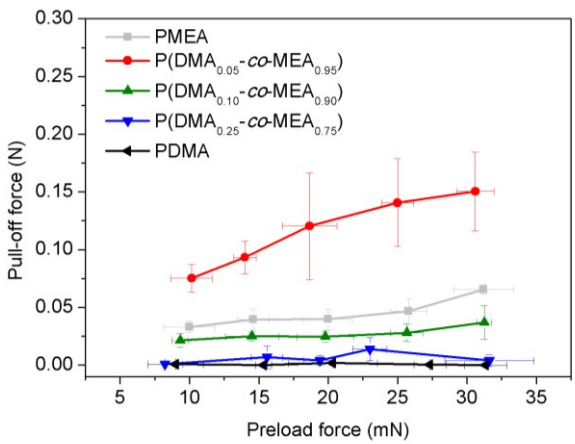

Figure 4. Pull-off forces under dry conditions as a function of preload force for (co)polymers with different DMA/MEA ratios. Probe speed was 0.01 mm/s for all measurements. Each data point resulted from an average of three to five measurements.

For most polymers, the adhesion force displayed a slight increase with increasing preload force. This trend is mainly due to the deeper indentation of the probe into the polymer film for higher preload force, resulting in a larger contact area and a higher strain. For a more viscoelastic material more energy will be dissipated leading to increased adhesion, thus the effect of preload is more pronounced for viscoelastic materials. However, in the current polymer system, polymers that are more viscoelastic, PMEA in particular, have a lower storage modulus and fewer branches (see Table 1). Polymers with a lower storage modulus and fewer branches feature lower cohesive strengths, which may reduce the effect of preload on pull-off force. Therefore, no large differences in preload dependence are obtained between the different polymers. The adhesion strength was obtained by dividing the adhesion force by the calculated contact area. The contact area A is obtained by calculating by $A = 2\pi R\delta$, where R is the radius of the glass probe, and δ is the indentation depth. The contact area is different for each preload force and each polymer (at the same preload force). Figure 5 presents the adhesion strength of the polymers at the same preload force of 13 mN and the calculated contact areas. It can be seen that the trend is the same as obtained in Figure 4. P($DMA_{0.05}$-*co*-$MEA_{0.95}$) exhibits the highest dry adhesion strength, and a further increase in DMA content in the polymer results in a significant decrease in adhesion.

The bulk mechanical properties determine the adhesive performance to a large extent. Typically, at a deformation rate of 1 Hz, the storage modulus for a pressure sensitive adhesive (PSA) lies within the range 10 – 300 kPa. In this range polymers are compliant enough to form good contact within the contact time and the debonding process is then determined by the coupling of bulk and interfacial properties of the material.[31] PMEA, P($DMA_{0.05}$-*co*-$MEA_{0.95}$) and P($DMA_{0.10}$-*co*-$MEA_{0.90}$) fall in this range, while P($DMA_{0.25}$-*co*-$MEA_{0.75}$) has a storage modulus of 4.8 x 10^4 kPa. PDMA is very brittle, and most likely exhibits a storage modulus that is even higher than P($DMA_{0.25}$-*co*-$MEA_{0.75}$). Therefore, P($DMA_{0.25}$-*co*-$MEA_{0.75}$) and PDMA are too stiff to be tacky. They will not be able to form a good contact with the probe and, thus, the interface can only support very limited deformation of the bulk. Tan δ/storage modulus is a measure for the strain the material can withstand before detachment will occur, this is indeed very low for P($DMA_{0.25}$-*co*-$MEA_{0.75}$).[32]

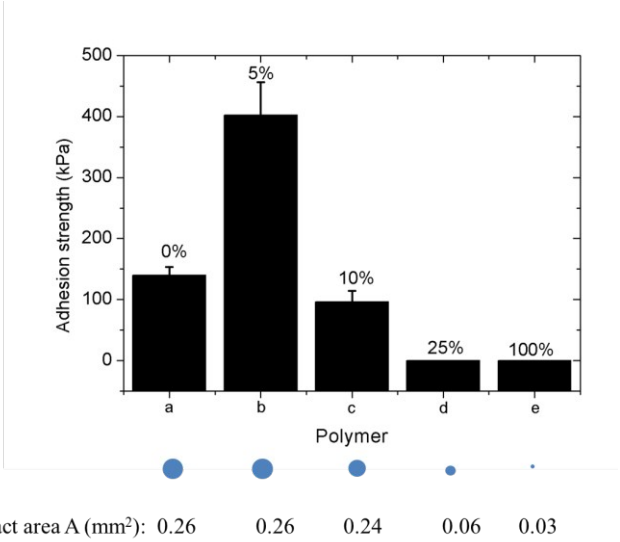

Figure 5. Adhesion strength of polymers at a preload force of 13 mN. The polymers are: a) PMEA, b) P($DMA_{0.05}$-*co*-$MEA_{0.95}$), c) P($DMA_{0.10}$-*co*-$MEA_{0.90}$), d) P($DMA_{0.25}$-*co*-$MEA_{0.75}$) and e) PDMA. The number on top of each bar is the molar percentage of DMA in the respective polymer. The standard errors were calculated based on three measurements for each sample.

In our study, the adhesion strength of P($DMA_{0.05}$-*co*-$MEA_{0.95}$) was 169% higher than that of PMEA. This increase can be explained by the property profile of the two polymers. First, although the storage modulus is low, PMEA is not cross-linked, leading to a low cohesive strength. This is also reflected in the fact that during the de-bonding process fibrils were formed between the PMEA film and the glass probe. Second, it has been reported that catechol can displace water molecules from wet silica and adheres strongly by hydrogen bonding.[33, 34] Third, the more hydrophobic monomer MEA as compared to DMA, will decrease the surface energy of the polymer. On a surface of high surface free energy such as the glass probe used in our measurement, a more hydrophilic polymer will exhibit a better wettability.[35] It is unclear why P($DMA_{0.10}$-*co*-$MEA_{0.90}$) shows much lower adhesion than P($DMA_{0.05}$-*co*-$MEA_{0.95}$) even though the DMechA experiments indicated very similar mechanical properties. It may be that during the DMechA experiment residual solvent was left in the sample, resulting in a measured storage modulus that is lower than the actual storage modulus of the polymer.

Effect of crosslinking on the dry adhesion

As becomes clear from the discussion above, it is difficult to draw conclusions about the influence of crosslinking in the polymers on the adhesion properties, because not only crosslinking, but also the T_g and *Mw* vary significantly between polymers. Therefore, one polymer, i.e. P($DMA_{0.05}$-*co*-$MEA_{0.95}$) that showed the best dry adhesion performance, was selected to study the influence of crosslinking.

To study the effect of crosslinking on dry adhesion, a certain amount of oxidant $NaIO_4$ was added to the polymer film to induce catechol oxidation and subsequent crosslinking. As shown in Figure 6, addition of small amounts of oxidant, i.e. $NaIO_4$/Catechol = 1/100 and $NaIO_4$/Catechol = 1/10, resulted in slightly reduced adhesion. A further increase in amount of oxidant, i.e. $NaIO_4$/Catechol = 1/3, resulted in negligible adhesion. These observations indicate that for P($DMA_{0.05}$-*co*-$MEA_{0.95}$) the addition of oxidant will always reduce adhesion. The reduction in adhesion may be due to changes at the interface and changes of the bulk properties: First, part of the catechols is oxidized to quinones, and quinones can lower the adhesion significantly.[8] Second, the oxidants will add crosslinks to the polymer systems which will lead to an increase in stiffness. Therefore, the crosslinked polymers are less tacky, resulting in reduced adhesion. Similar observations have been reported by Washburn et al. [20], who studied the dry adhesion of copolymer poly(DMA-*co*-MEA) containing 12 mol% DMA by adding a divinyl cross-linking agent.

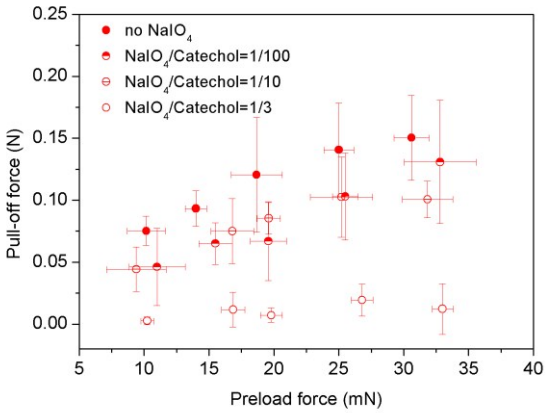

Figure 6. Dry adhesion of P($DMA_{0.05}$-*co*-$MEA_{0.95}$) in the presence of an oxidant $NaIO_4$. Each data point resulted from an average of three to five measurements.

Wet adhesion

For the wet adhesion in aqueous conditions at pH 3, the polymer films were fully immersed in aqueous HCl at pH 3 for at least one hour to equilibrate the water uptake into the polymer. Measurements were performed at pH 3 due to the sensitivity of catechol to oxidation at moderate to high pH. Oxidation of the catechols may influence the adhesion performance.[36]

As shown in Figure 7, the adhesion force for PMEA, P($DMA_{0.05}$-*co*-$MEA_{0.95}$) and P($DMA_{0.10}$-*co*-$MEA_{0.90}$) under wet conditions is lower than for dry adhesion. It is interesting to note that P($DMA_{0.25}$-*co*-$MEA_{0.75}$) showed considerable wet adhesion, but almost no dry adhesion. PDMA showed negligible wet adhesion. The effect of DMA content on wet adhesion followed a similar trend as for dry adhesion: Incorporation of 5 mol% of DMA in the copolymer resulted in enhanced wet adhesion. A further increase in DMA content reduced the wet adhesion significantly. A different trend was observed by Butt and coworkers.[37] They investigated the single-molecular wet adhesion of poly(dopamine methacrylamide-*co*-butylamine methacrylamide), and observed an independence of catechol content on wet adhesion. However, single-molecule force measurements differ from macroscopic adhesion measurements and different properties are assessed.

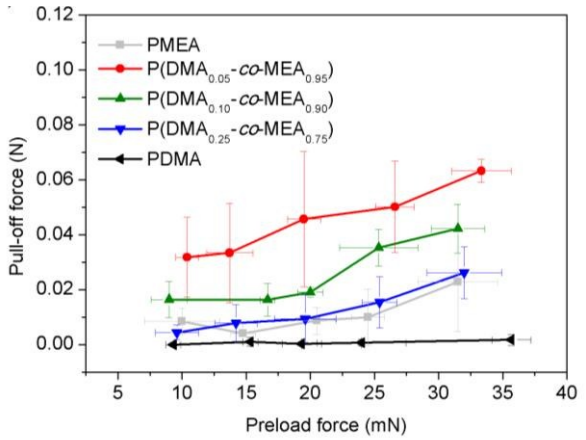

Figure 7. Pull-off forces under wet conditions as a function of preload force for (co)polymers with different DMA/MEA ratios. Probe speed was 0.01 mm/s for all measurements. Each data point resulted from an average of three to five measurements.

Compared to dry adhesion, the decreased adhesion under wet conditions may be due to weaker surface interactions. To investigate the difference in mechanical properties of the polymer films between dry and wet conditions, the compressive parts of the force-displacement curves, i.e. the linear part of the approaching step, were analyzed using the Hertz theory of elastic contact.[38] The Hertzian indentation model can be expressed as:

$$P = \frac{3}{4}E^*\sqrt{R\delta^3} \qquad (2)$$

where P is the preload force, $E^* = E/(1-\upsilon^2)$ is the effective Young's modulus of the surface, υ is Possion's ratio, R is the radius of the indentation sphere, and δ is the indentation depth. Table 3 shows E^* for all polymers obtained from Hertz theory under both dry and wet conditions. Since some of the polymers display significant viscoelastic effects, the model has limited applicability and the E^* values are only used to compare the differences in stiffness of polymers under dry and wet conditions.

Table 3. Changes in stiffness of the five polymers under wet and dry conditions

	Stiffness (N/mm^2)		
	Dry	Wet	Δ^a
PMEA	11	5.2	5.8
P(DMA$_{0.05}$-*co*-MEA$_{0.95}$)	19.4	9.5	9.9
P(DMA$_{0.10}$-*co*-MEA$_{0.90}$)	31.2	18	13.2
P(DMA$_{0.25}$-*co*-MEA$_{0.75}$)	47	27	20
PDMA	48	38	10

Under dry conditions, an increase in stiffness was obtained with increasing DMA content in the polymer. Under wet conditions, all polymers showed a significantly lower stiffness than the stiffness under dry conditions. The decrease in stiffness (Δ) was more pronounced for polymers with a higher DMA content, except for PDMA. Whitening of the polymers was observed upon immersion indicating swelling with water. Water acts as a plasticizer, lowering the T_g and the stiffness of the polymer films. DMA is a more hydrophilic monomer than MEA. Therefore, when more DMA is incorporated, the polymer is swollen to a larger extent compared to polymers containing less DMA. In PDMA swelling may be limited due to the crosslinked nature of the polymer. For P(DMA$_{0.10}$-*co*-MEA$_{0.90}$), and P(DMA$_{0.25}$-*co*-MEA$_{0.75}$), the swollen films become more compliant, which results in a better contact with the probe. Therefore, a relatively higher adhesion under wet conditions than under dry conditions is obtained as compared to the other compositions.

Conclusions

We synthesized poly(DMA-*co*-MEA) copolymers with different compositions and found an increase in the degree of crosslinking by increasing the catechol content in the polymer. The effect of catechol content on the adhesion properties was studied and an optimal composition for dry adhesion was achieved at a DMA concentration of 5 mol%. Polymers with a higher concentration of DMA showed little dry adhesion, which is attributed to the high stiffness of the material, resulting in poor contact with the probe. The adhesion properties of the polymer under dry conditions are a balance between catechol content to strengthen the interface, compliance to ensure good contact formation and a small degree of crosslinking to increase cohesion.

Under wet conditions, the copolymers showed a similar dependence on the DMA composition as compared to dry conditions. An optimal composition for the best wet adhesion was found at a DMA concentration of 5 mol%. Polymers with a higher DMA content are more hydrophilic and will take up more water. As water acts as a plasticizer and reduces the effective stiffness, polymers with a higher DMA content will show a larger decrease in stiffness, which improved their wet adhesion performance.

Acknowledgements

We would like to thank Dr. Frank Snijkers for help with rheology measurements; Wouter Teunissen for help with SEC-MALLS measurements and Herman de Beukelaer for help with DSC measurements.

Notes and references

[a] Laboratory of Physical Chemistry and Colloid Science, Wageningen University, Dreijenplein 6, 6703 HB Wageningen, the Netherlands
[b] Akzo Nobel Decorative Coatings B.V., Rijksstraatweg 31, 2171 AJ Sassenheim, The Netherlands

Electronic Supplementary Information (ESI) available. See DOI: 10.1039/b000000x/

1. J. H. Waite, *Biol. Rev.*, 1983, **58**, 209-231.
2. J. H. Waite, T. J. Housley and M. L. Tanzer, *Biochemistry*, 1985, **24**, 5010-5014.
3. H. Zhao, C. J. Sun, R. J. Stewart and J. H. Waite, *J. Biol. Chem.*, 2005, **280**, 42938-42944.

4. J. H. Waite, R. A. Jensen and D. E. Morse, *Biochemistry*, 1992, **31**, 5733-5738.
5. J. H. Waite, *Polym. Prepr.*, 1990, **30**, 181-182.
6. H. J. Meredith, C. L. Jenkins and J. J. Wilker, *Advanced functional materials*, 2014, **24**, 3259–3267.
7. H. Lee, N. F. Scherer and P. B. Messersmith, *Proceedings of the National Academy of Sciences of the United States of America*, 2006, **103**, 12999-13003.
8. J. Yu, W. Wei, E. Danner, J. N. Israelachvili and J. H. Waite, *Advanced materials*, 2011, **23**, 2362-2366.
9. Q. Ye, F. Zhou and W. M. Liu, *Chem. Soc. Rev.*, 2011, **40**, 4244-4258.
10. C. L. Frye, *J. Am. Chem. Soc.*, 1964, **86**, 3170-3171.
11. Q. Lin, D. Gourdon, C. J. Sun, N. Holten-Andersen, T. H. Andersen, J. H. Waite and J. N. Israelachvili, *Proceedings of the National Academy of Sciences of the United States of America*, 2007, **104**, 3782.
12. J. L. Dalsin, L. J. Lin, S. Tosatti, J. Voros, M. Textor and P. B. Messersmith, *Langmuir*, 2005, **21**, 640-646.
13. E. Faure, C. Falentin-Daudré, C. Jérôme, J. Lyskawa, D. Fournier, P. Woisel and C. Detrembleur, *Progress in Polymer Science*, 2013, **38**, 236-270.
14. C. R. Matos-Perez, J. D. White and J. J. Wilker, *Journal of the American Chemical Society*, 2012, **134**, 9498-9505.
15. M. Guvendiren, D. A. Brass, P. B. Messersmith and K. R. Shull, *The Journal of Adhesion*, 2009, **85**, 631-645.
16. N. Schweigert, A. J. B. Zehnder and R. I. L. Eggen, *Environmental Microbiology*, 2001, **3**, 81-91.
17. V. Thavasi, R. P. A. Bettens and L. P. Leong, *J Phys Chem A*, 2009, **113**, 3068-3077.
18. H. Lee, B. P. Lee and P. B. Messersmith, *Nature*, 2007, **448**, 338-341.
19. P. Glass, H. Chung, N. R. Washburn and M. Sitti, *Langmuir*, 2009, **25**, 6607-6612.
20. H. Chung, P. Glass, J. M. Pothen, M. Sitti and N. R. Washburn, *Biomacromolecules*, 2011, **12**, 342-347.
21. H. Shao and R. J. Stewart, *Advanced materials*, 2010, **22**, 729-733.
22. H. Shao, K. N. Bachus and R. J. Stewart, *Macromolecular Bioscience*, 2009, **9**, 464-471.
23. H. Shao, G. M. Weerasekare and R. J. Stewart, *J. Biomed. Mater. Res., Part A*, 2011, **97**, 46-51.
24. B. P. Lee, K. Huang, F. N. Nunalee, K. R. Shull and P. B. Messersmith, *J Biomat Sci-Polym E*, 2004, **15**, 449-464.
25. C. Creton, G. J. Hu, F. Deplace, L. Morgret and K. R. Shull, *Macromolecules*, 2009, **42**, 7605-7615.
26. J. Yang, M. A. Cohen Stuart and M. Kamperman, *Chem. Soc. Rev.*, 2014, **43**, 8271-8298.
27. J. Cazes, ed., *Encyclopedia of Chromatography*, Marcel Dekker Inc 2005.
28. G. Hohne, W. F. Hemminger and H. J. Flammersheim, *Differential Scanning Calorimetry*, Springer, 2003.
29. L. A. Burzio and J. H. Waite, *Biochemistry*, 2000, **39**, 11147-11153.
30. C. Gabriel, E. Kokko, B. Lofgren, J. Seppala and H. Miinstedt, *Polymer*, 2002, **43**, 6383.
31. A. V. Pocius, *Adhesion and adhesives technology: an introduction*, Carl Hanser Verlag, München, 2012.
32. C. Creton, F. J. Hu and F. Deplace, *Macromolecules*, 2009, **42**, 7605-7615.
33. S. A. Mian, X. F. Gao, S. Nagase and J. Jang, *Theor Chem Acc*, 2011, **130**, 333-339.
34. S. A. Mian, L. C. Saha, J. Jang, L. Wang, X. F. Gao and S. Nagase, *J. Phys. Chem. C*, 2010, **114**, 20793-20800.
35. H. Yamamoto, Y. Sakai and K. Ohkawa, *Biomacromolecules*, 2000, **1**, 543-551.
36. B. P. Lee, C. Y. Chao, F. N. Nunalee, E. Motan, K. R. Shull and P. B. Messersmith, *Macromolecules*, 2006, **39**, 1740.
37. J. Wang, M. N. Tahir, M. Kappl, W. Tremel, N. Metz, M. Barz, P. Theato and H.-J. Butt, *Advanced materials*, 2008, **20**, 3872-3876.
38. H. Hertz, *J. Reine Angew. Math.*, 1882, **92**, 156-171.